Hindawi Publishing Corporation
Journal of Spectroscopy
Volume 2015, Article ID 736382, 9 pages
http://dx.doi.org/10.1155/2015/736382

Research Article

Retrieval of Atmospheric CO_2 and CH_4 Variations Using Ground-Based High Resolution Fourier Transform Infrared Spectra

Tian Yuan,[1] Liu Cheng,[1,2] Sun You Wen,[1] Xie Pin Hua,[1,2] Wang Wei,[1] Liu Wen Qing,[1,2] Liu Jian Guo,[1,2] Li Ang,[1] Hu Ren Zhi,[1] and Zeng Yi[1]

[1]*Key Lab of Environmental Optics & Technology, Anhui Institute of Optics and Fine Mechanics, Chinese Academy of Sciences, Hefei 230031, China*
[2]*University of Science and Technology of China, Hefei 230026, China*

Correspondence should be addressed to Liu Cheng; liucheng@hfcas.ac.cn

Received 23 June 2015; Accepted 31 August 2015

Academic Editor: Arnaud Cuisset

High resolution Fourier transform near IR solar spectra are used to estimate the column-averaged dry-air mole fraction (DMF) of CO_2 and CH_4 variations in the atmosphere. The preliminary retrieval results for CO_2 and CH_4 variations in the area of Hefei, China, are presented, and the underlying error sources are also analyzed. Both a forward analysis and an inversion algorithm are included in the retrieval. The forward analysis uses the modeled atmospheric transmittance to line-by-line (LBL) convolute the instrument line shape function. The influences of the temperature, pressure, humidity, and a priori gases are considered in the atmospheric transmittance model. The inversion algorithm is based on the nonlinear iterative and nonlinear least squares spectral fitting, which is used to obtain VCD_{CO_2} and VCD_{CH_4} (which represent vertical column density of CO_2 and CH_4, resp.). Furthermore, the VCD_{O_2} is also retrieved for converting the VCDs into DMFs. DMFs are final products of data analysis. The inversion results can clearly resolve the tiny variations of CO_2 and CH_4 under strong atmospheric background. Spectral fitting residuals for both VCD_{CO_2} and VCD_{CH_4} are less than 0.5%. Finally, CO_2 and CH_4 diurnal variations are investigated based on a typical observation. About 2 ppm amplitude for DMF_{CO_2} diurnal variations and less than 15 ppb amplitude for DMF_{CH_4} are observed.

1. Introduction

Greenhouse effect caused by greenhouse gases (GHGs) can produce a series of environmental and economic problems. Recording GHG variations with high precision and accuracy is of great significance for predicting future climate change. Besides, good knowledge of global source and sink of carbon is the prerequisite for global warming control because carbon (except vapor) is the most important component in the GHGs [1].

CO_2 and CH_4 are two important GHGs and carbon compounds, which have been the research hotspots for decades [1, 2]. To have good knowledge of these two gases, the world has established more than 100 in situ observation sites over the past 30 years [3, 4]. A large number of GHG researches have been accomplished based on the combination of the in situ observation and global transmission model. In situ observations are mainly focused on the atmospheric boundary layer. The most striking characteristic of in situ observations on the atmospheric boundary layer is its high accuracy. But it is severely affected by the local source and sink and limited in the spatial coverage range [5]. Column density measurements can fill these gaps and are less influenced by the atmospheric boundary layer height changes and vertical transport [6]. Compared to in situ observation, column density measurements are less affected by temporal and spatial variations and thus make the horizontal gradients of the results more directly related to the underlying regional-scale fluxes [5]. The typical high precision tools for column measurements are satellite-based and ground-based Fourier transform spectrometer [7]. Currently, satellite-based Fourier transform spectrometer includes GOSAT (Japan), launched

(a) Indoor (b) Outdoor

Figure 1: Experimental instrument system.

in 2009, and the OCO-2 (United States), launched in 2014. To validate these satellite data, ground-based atmospheric GHGs observation network is established, called the Total Carbon Column Observation Network (TCCON) [5]. However, there is still no TCCON site locating in the area of China. That means it is unable to validate the satellite-based measurements in the whole area of China.

This paper aims to first retrieve CO_2 and CH_4 variations in China using ground-based high resolution Fourier transform infrared spectra. This study can not only provide an evidence for resolving the local source and sink of carbon circle but also facilitate the satellite-based GHG measurements validation.

2. Instrument Descriptions

The observation laboratory is installed on an island located in the west of Hefei (the capital of Anhui Province) in central and eastern China. It is adjacent to a lake with a longitude of 117°10′E, latitude of 31°54′N, and altitude of 30 m. The system consists of a high resolution ground-based Fourier transform infrared spectrometer (IFS125HR) and a solar tracker (Tracker-A Solar 547), both of which are purchased from Bruker Company. IFS125HR has 9 scanner compartments, with a maximum resolution of 0.00096 cm^{-1}, and covers a spectral range of 5~50,000 cm^{-1}. The solar tracker is mounted inside a dome controlled by a motor on the building roof (as shown in pictures on the right of Figure 1). A tracking precision of ±0.1° can be achieved by using the Camtracker mode (a built-in camera continuously adjusts the distance between the sun spot and the field spot). Solar tracker directs the sun light through the roof aperture (as shown in pictures on the left of Figure 1) into the spectrometer. For CO_2 and CH_4 observation, the spectral resolution is set to 0.02 cm^{-1} and the CaF_2 beam splitter is used [8]. We choose InSb as the detector which covers 3900~15500 cm^{-1} spectral range and cooled with liquid nitrogen during operation. In order to avoid detector saturation, we select a minimum entrance aperture (0.5 mm) and insert an attenuator (grid metal) in front of the detector.

3. Spectra Retrieval

Spectra retrieval includes two steps, that is, VCDs retrieval and then DMFs retrieval. We use the GFIT algorithm to retrieve the CO_2 and CH_4 VCDs. GFIT is developed by JPL (Jet Propulsion Laboratory), California Institute of Technology [5, 9]. It combines nonlinear iteration and nonlinear least squares fitting. It is a standard inversion algorithm for TCCON network. When fitting a spectral range, GFIT attempts to minimize the quantity χ^2 with respect to the variables α, β, δ, x_1, x_2, and x_3 and other parameters:

$$\chi^2 = \sum_{i=1}^{NM} \frac{\left(Y_i^M - Y^C\left(\alpha, \beta, V_i + \delta, x_1, x_2, x_3 \cdots\right)\right)^2}{\delta_i^2}, \quad (1)$$

where Y^M represents the measured spectra, Y^C represents the calculated spectra, α is termed the continuum level, β is termed the continuum tilt, δ is the frequency shift, and the

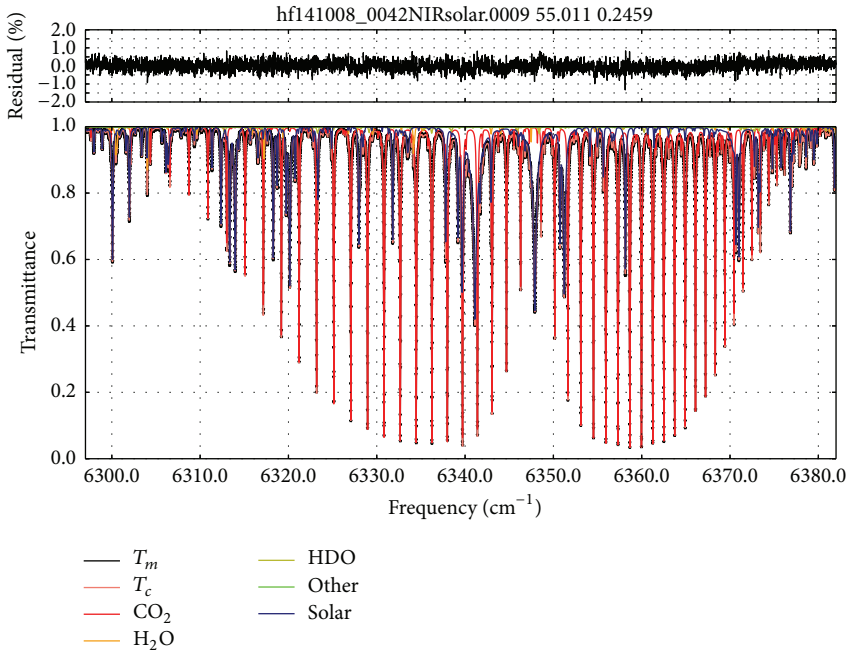

FIGURE 2: CO_2 spectral fitting within 6339 cm^{-1} window: the spectrum was recorded on October 8, 2014, 0:47 (UTC). Black lines are the measurements, orange lines are the fitted transmittance, and contributions from individual gases are shown in color. Fitting residuals ($T_m - T_c$) for CO_2 are 0.2459%.

various x terms are the scale factors for the different gases and σ_i is the uncertainty in the value of the ith element of Y^M. α, β, δ, x_1, x_2, x_3, . . ., and so forth are important outputs of GFIT. Due to the complexity of modeling the measured spectra Y^M, a forward model Y^C is exploited. It is expressed as

$$Y^M = Y^C + \varepsilon, \tag{2}$$

where ε is the measurement error.

Forward model Y^C is commonly termed the convolution of atmospheric transmittance and the instrument line shape function [10, 11]:

$$y_i^c = \left\{\left[C + S\left(\nu_i - \nu_0\right)\right] y_{i_{\text{top}}} \text{ILS}\left(\nu_i, \delta\right) \otimes T\left(\nu_i\right)\right\} + z_{\text{offset}}, \tag{3}$$

$$T\left(\nu_i\right) = e^{-\sum_{j=0}^{70} \sum_k^K \sum_l^L \{[c_k w_{0k,j}][R_{l,k,j} F_{l,k,j}(\nu_i - \nu_{k,j})] n_j s_j\}}, \tag{4}$$

where y_i^c is the ith element of Y^C, $y_{i_{\text{top}}}$ is the atmosphere top layer spectra, C is continuum level, S is continuum tilt, δ is frequency drift, and $T(\nu_i)$ represents atmospheric transmittance. When modeling measured spectra, a discrete, line-by-line, multilayer, and multispecies expression for the atmospheric transmittance is applied as expressed by (4) [5]. ν_0 is the center frequency of a spectral window, ILS(ν_i, δ) is instrument line shape function, and z_{offset} is spectral zero level offset. And the ILS used in GFIT is a nominal ideal ILS that is a numerical convolution of the sinc function with a rectangular function when the instrument is well aligned. The effect of the thermal radiation is ignored due to its negligible influence on the near-infrared spectrum. Solar intensity relative fluctuation threshold is set to 5% for removing the interference of clouds and aerosols.

3.1. Model Parameters Determination. In order to achieve high precision retrieval, longitude, latitude, altitude, a priori profiles, real-time surface temperature, humidity, pressure, wind speed, wind direction, and other meteorological parameters need to be considered in the process of the forward model calculation [12]. In addition, the high resolution spectrometer IFS125HR should be calibrated by a low pressure HCl cell regularly because instrument alignment has great influence on the inversion results [10]. For the current version of spectra, we did not save the real-time surface temperature, humidity, and pressure parameters, and no HCl cell is available. Thus, in this study, we have to make some assumptions in the model calculation.

(1) Inside the laboratory, the air conditioning is set to a constant value of 24°, the dehumidifier is set to a constant value of 60%, and the IFS125HR is evacuated while saving the solar spectra. So we assume that the temperature inside the instrument (T_{inside}) is a constant value of 24°, the internal pressure (P_{inside}) is a constant value of 1 mbar, the internal relative humidity (H_{inside}) is a constant value of 60%, the temperature outside the instrument (T_{outside}) is a constant value of 24°, the external pressure (P_{outside}) is a constant value of 1 standard atmospheric pressure (1024 pa), and the external relative humidity (H_{outside}) is a constant value of 60%. In addition, a priori profiles for temperature, pressure, and humidity above observation station are based on NCEP (National Center for Environmental Prediction) data [13]. A priori profiles for all gases use the American standard

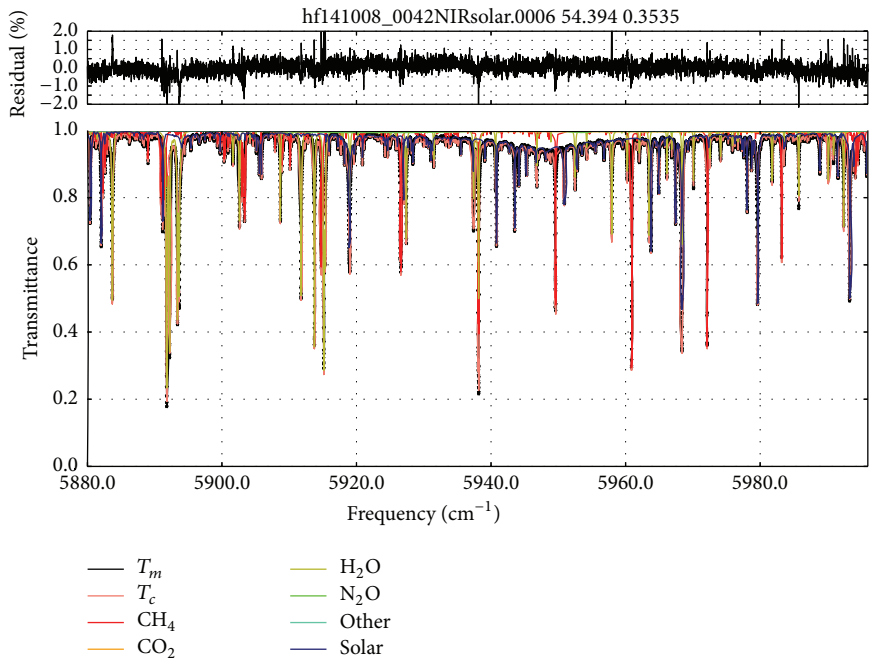

FIGURE 3: CH_4 spectral fitting within 5938 cm^{-1} window: the spectrum was recorded on October 8, 2014, 0:47 (UTC). Black lines are the measurements, orange lines are the fitted transmittance, and contributions from individual gases are shown in color. Fitting residuals ($T_m - T_c$) for CH_4 are 0.3535%.

atmospheric parameters for the mid-latitude of northern hemisphere.

(2) We already aligned the IFS125HR just before we started to save the spectra, so we assume that the alignment of instrument is well because of the excellent stability of the instrument; that is, the influence of the instrument drift is neglected for all the spectra.

(3) Time correction is done every day before observations, so the saved spectra are consistent with the UTC (Universal Time Coordinated) within ±1-second precision.

3.2. VCD Retrieval. We use the GFIT algorithm to calculate the CO_2 and CH_4 VCDs which finds the best fitting between the calculated spectra and the measured spectra [14]. The most important outputs of the GFIT algorithm are scaling factors and their uncertainties as mentioned in (1). A priori profile mole fraction of a gas is multiplied by the scaling factor to yield the retrieved vertical column density [13]

$$\text{column}_{\text{gas}} = \text{SF}_{\text{gas}} \int_{z_s}^{\infty} f_{\text{gas}}^{\text{apriori}} n \, dz, \tag{5}$$

where SF_{gas} is the scaling factor for a gas, $f_{\text{gas}}^{\text{apriori}}$ is the a priori profile of the gas, n is the total molecules number, z represents altitude, and z_s is the altitude of the first mirror of the solar tracker.

3.3. DMF Calculation. Gas column average dry-air mole fraction (DMF) is defined as

$$X_{\text{gas}} = \frac{\text{column}_{\text{gas}}}{\text{total dry column}}. \tag{6}$$

Because VCD_{O_2} in the atmosphere is well known, the total dry-air column can be obtained by using the relationship between VCD_{O_2} and the total dry-air column [15]:

$$\text{total dry column} = \frac{\text{column}_{O_2}}{0.2095}. \tag{7}$$

Substituting (7) into (6) yields the DMF:

$$X_{\text{gas}} = 0.2095 \frac{\text{column}_{\text{gas}}}{\text{column}_{O_2}}. \tag{8}$$

The advantages of DMF compared with VCD are as follows: (1) reducing the influence of surface pressure changes and water vapor interference on the inversion results; (2) reducing the systematic error sources which affect both the target gas and O_2; (3) improving the inversion precision by minimizing the common scatter [15].

4. Data Analysis and Discussion

In this study, the direct solar spectra collected between October 6, 2014, and December 1, 2014, are retrieved. All the spectra which are saturated or the signal to noise ratios (SNR) which are less than 500 or the relative intensity variations which are larger than 5% (mainly caused by clouds and/or aerosols) are removed. CO_2, CH_4, and O_2 gases are retrieved simultaneously. Retrieval window parameters for CO_2, CH_4, and O_2 are listed in Table 1. The two central frequencies for CO_2 windows are 6220.00 cm^{-1} and 6339.50 cm^{-1}, respectively. The final VCD_{CO_2} is the average of the windows' results. The same treatment is also applied to CH_4. The target gases

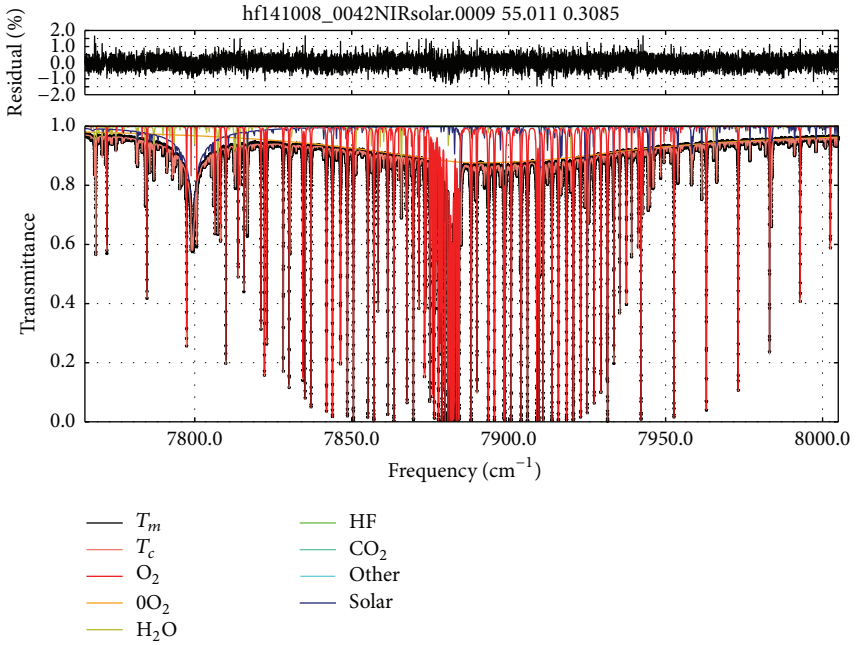

FIGURE 4: O_2 spectral fitting within 7885 cm^{-1} window: the spectrum was recorded on October 8, 2014, 0:47 (UTC). Black lines are the measurements, orange lines are the fitted transmittance, and contributions from individual gases are shown in color. Fitting residuals ($T_m - T_c$) for O_2 are 0.3085%.

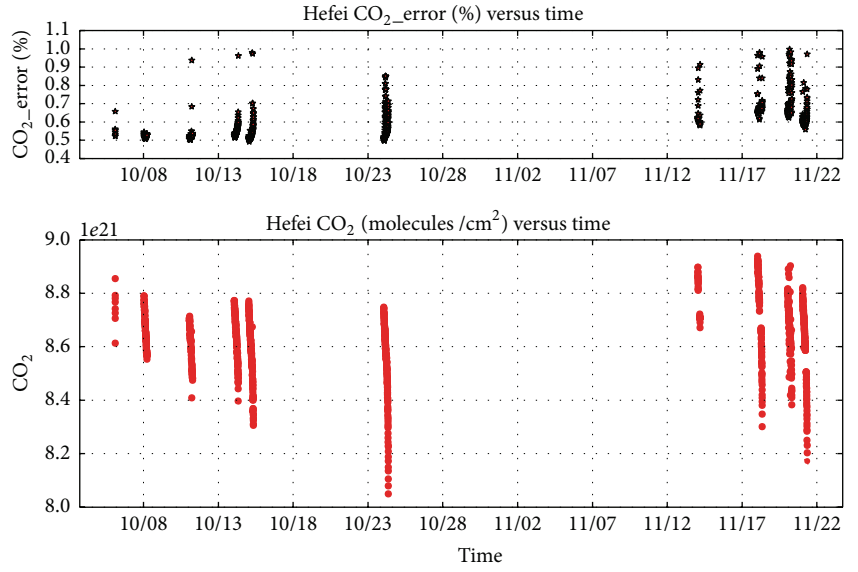

FIGURE 5: VCD_{CO_2} time series ranging from October 6, 2014, to December 1, 2014, which are the average of the retrieval values in 6220 cm^{-1} and 6339 cm^{-1} windows.

of interest (bold font) and interfering gases are also shown in Table 1. We set a fitting residual of <1% to filter out those spectra which do not fulfill the assumptions in Section 3.1.

Figures 2, 3, and 4 are fitting examples for CO_2, CH_4, and O_2, respectively, which are from a spectrum measured at 26.535° SZA (solar zenith angle) on October 8, 2014. T_c and T_m represent calculated spectrum and measured spectrum, respectively. Fitting residuals ($T_m - T_c$) for CO_2, CH_4, and O_2 are 0.2459%, 0.3535%, and 0.3085%, respectively. The fitting residuals are mainly attributed to the unknown structure of spectroscopies and systematic errors, for example, electronic noise, acquisition noise, spectral structure noise, and scanning mirror fluctuation noise.

The time series of retrieved VCD_{CO_2} and VCD_{CH_4} are shown in Figures 5 and 6, respectively. Time periods ranging from October 6, 2014, to December 1, 2014, are presented for

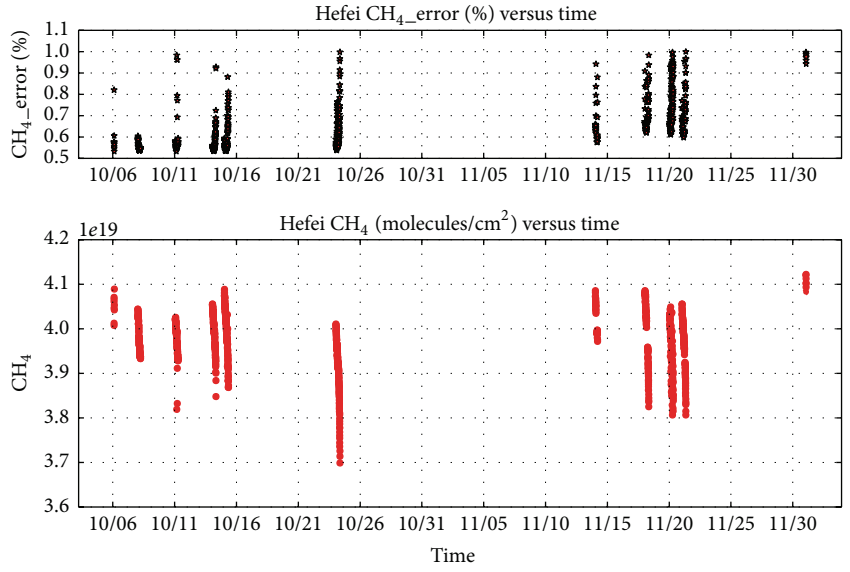

Figure 6: VCD_{CH_4} time series ranging from October 6, 2014, to December 1, 2014, which are the average of the retrieval values in 5938 cm^{-1}, 6002 cm^{-1}, and 6076 cm^{-1} windows.

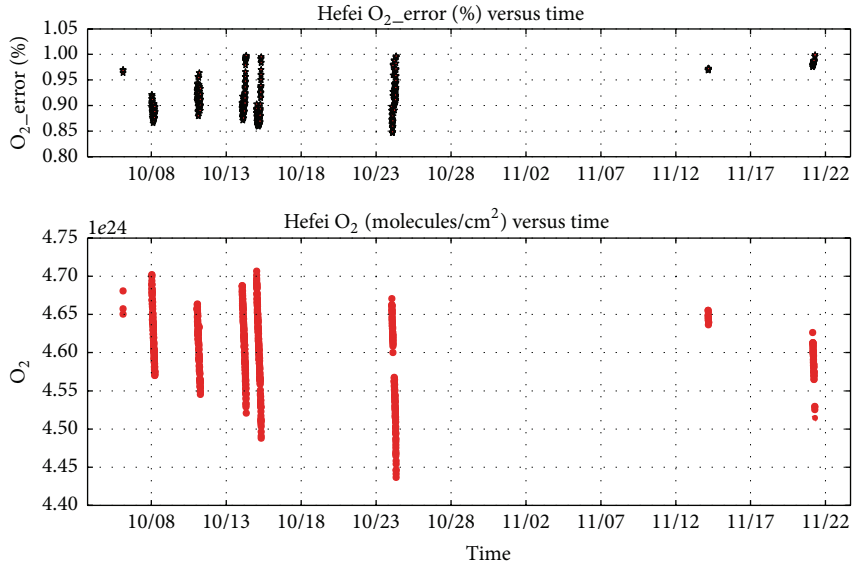

Figure 7: VCD_{O_2} time series ranging from October 6, 2014, to December 1, 2014, which are the retrieval values in 7885 cm^{-1} window.

Table 1: Retrieval window parameters for CO_2, CH_4, and O_2.

Gases to fit	Central frequencies (cm^{-1})	Width (cm^{-1})
CO_2, H_2O, HDO, and CH_4	6220.00	80.00
CO_2, H_2O, and HDO	6339.50	85.00
CH_4, CO_2, H_2O, and HDO	5938.00	116.00
CH_4, CO_2, H_2O, and HDO	6002.00	11.10
CH_4, CO_2, H_2O, and HDO	6076.00	138.00
O_2, CO_2, H_2O, and HF	7885.00	240.00

both CO_2 and CH_4. The VCD_{CO_2} in Figure 5 is the average of the fitted results in 6220 and 6339 windows. The averaged fitting errors for CO_2 are less than 1%. Most VCD_{CO_2} lies between 8.2 and 8.8 $\times$ 10^{21} molecules/cm^2. The VCD_{CH_4} in Figure 6 is the average of the results in 5938 cm^{-1}, 6002 cm^{-1}, and 6076 cm^{-1} windows. Most VCD_{CH_4} lies between 3.7 and 4.1 $\times$ 10^{19} molecules/cm^2. The averaged fitting errors for CH_4 are also less than 1%. Figure 7 is the VCD_{O_2} time series retrieved from 7885 cm^{-1} window with fitting error of <1%. VCDs as shown in Figures 5~7 are intermediate products of data analysis and so postprocessing procedures

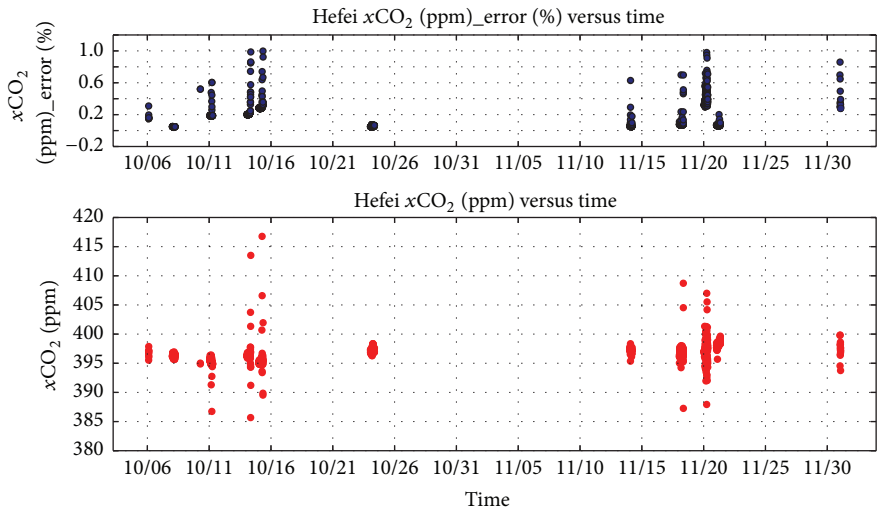

FIGURE 8: DMF_{CO_2} time series ranging from October 6, 2014, to December 1, 2014, which are calculated according to VCD_{CO_2} and VCD_{O_2}.

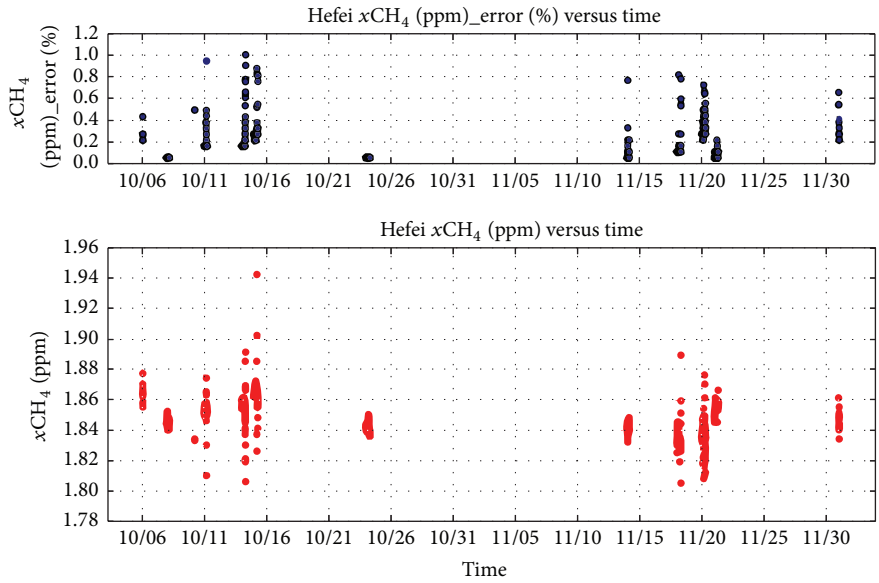

FIGURE 9: DMF_{CH_4} time series ranging from October 6, 2014, to December 1, 2014, which are calculated according to VCD_{CH_4} and VCD_{O_2}.

are not applied to them. Time series of DMF_{CO_2} and DMF_{CH_4}, respectively, in Figures 8 and 9 are calculated by the ratio of VCD_{CO_2}/VCD_{O_2} and VCD_{CH_4}/VCD_{O_2}, respectively. DMFs are final products of the data analysis. Both retrieval errors and precision are improved greatly (with less scatters).

In addition, the diurnal variations of DMF_{CO_2} and DMF_{CH_4} are investigated based on typical daily measurements. The diurnal variations of both DMF_{CO_2} and DMF_{CH_4} are clearly observed, which are shown in Figures 10 and 11, respectively. Precision (1σ standard error) for both DMF_{CO_2} and DMF_{CH_4} is less than 0.1%. DMF_{CO_2} concentrates on around 396 ppmv with diurnal variation amplitude of ~ 2 ppm. DMF_{CH_4} concentrates on around 1845 ppbv with diurnal variation amplitude of ~15 ppbv. The peak in DMF_{CO_2} and DMF_{CH_4} on October 24, 2014, may be caused by human activities. The observed diurnal variations do not indicate any feature so far, but with the increase of the number of observations we will do further research.

5. Conclusions and Discussion

CO_2 and CH_4 are important greenhouse gases and carbon compounds. Capturing their variations in the atmosphere is of importance to determine their source or sink information. This study uses high resolution Fourier transform near IR solar spectra to calculate the CO_2 and CH_4 VCDs and DMFs. The preliminary retrieval results for CO_2 and CH_4 variations in the area of Hefei, China, are presented, and the underlying error sources are also analyzed. The results show that tiny variations of CO_2 and CH_4 in the atmosphere can be clearly resolved. The retrieval error is dominated by the deficiencies in the forward model. Future work will concentrate on

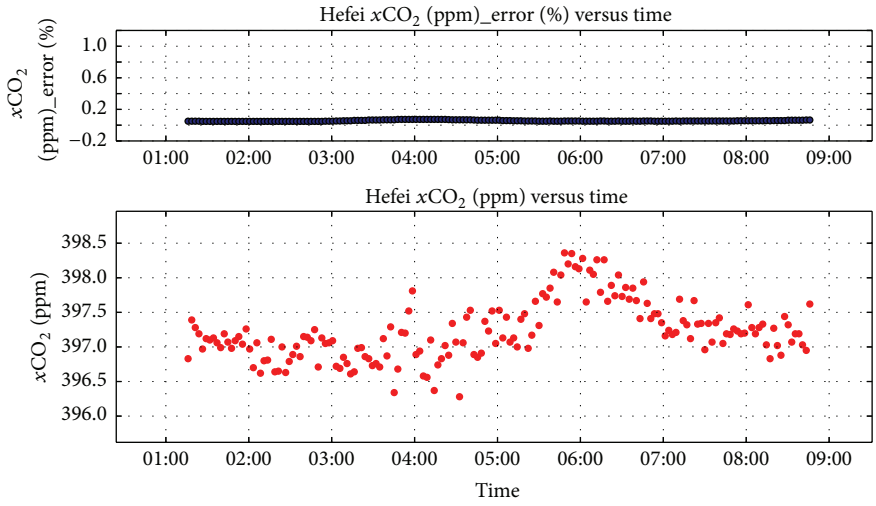

FIGURE 10: DMF_{CO_2} time series on October 24, 2014, which are calculated according to VCD_{CO_2} and VCD_{O_2}.

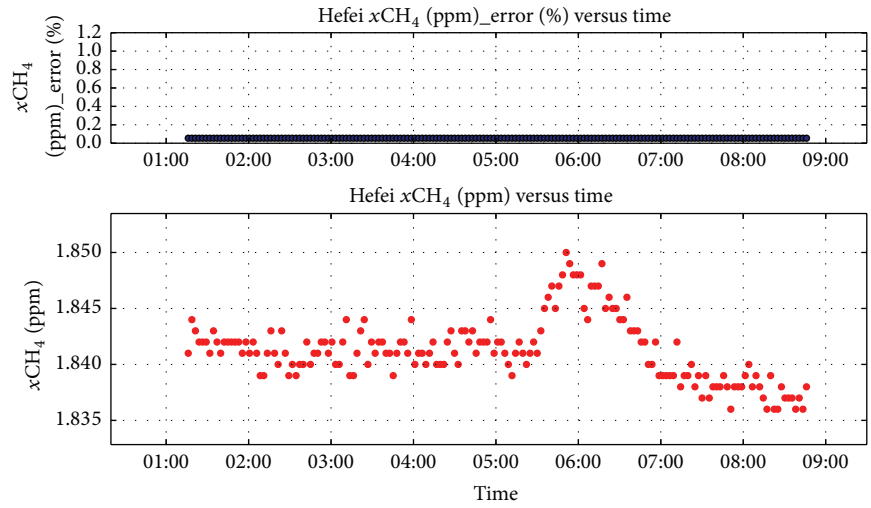

FIGURE 11: DMF_{CH_4} time series on October 24, 2014, which are calculated according to VCD_{CH_4} and VCD_{O_2}.

optimizing the input parameters of the model and calibrate the instrument regularly with HCl cell. We are confident that, with these improvements, this technical will be more than adequate for future climate change forecast and satellite-based column observations validation.

Conflict of Interests

The authors declare that there is no conflict of interests regarding the publication of this paper.

Acknowledgments

This work is jointly supported by the National Natural Science Foundation of China (Grant no. 41275038), the Key Research Program of the Chinese Academy of Sciences (Grant no. KJZD-EW-TZ-G06), the National High Technology Research and Development Program of China (Grants nos. 2014AA06A508 and 2014AA06A511), the Scientific and Technological Project of Anhui Province (Grant no. 1301022083), and the Natural Science Foundation of Anhui Province (Grant no. 1308085QF124). The authors would like to thank Caltech JPL for providing the source code of GFIT which formed the basis of the retrieval program in this study. They also give great thanks to Bremen IUP for assisting in the spectra retrieval.

References

[1] R. J. Andres, G. Marland, and S. Bischof, *Global and Latitudinal Estimates of δ13C from Fossil-Fuel Consumption and Cement Manufacture*, Carbon Dioxide Information Center, Oak Ridge National Laboratory, Oak Ridge, Tenn, USA, 1999, ftp://cdiac.ornl.gov/pub/db1013/.

[2] GLOBALVIEW-CO2: Cooperative Atmospheric Data Integration Project 21 Carbon Dioxide, CDROM, NOAA ESRL, Boulder, Colo, USA, 2009, ftp://ftp.cmdl.noaa.gov/products/globalview/co2/.

[3] F. Chevallier, N. M. Deutscher, T. J. Conway et al., "Global CO_2 fluxes inferred from surface air-sample measurements and from TCCON retrievals of the CO_2 total column," *Geophysical Research Letters*, vol. 38, no. 24, pp. 1–5, 2011.

[4] T. Warneke, A. K. Petersen, C. Gerbig et al., "Co-located column and in situ measurements of CO_2 in the tropics compared with model simulations," *Atmospheric Chemistry and Physics*, vol. 10, no. 12, pp. 5593–5599, 2010.

[5] D. Wunch, G. C. Toon, J.-F. L. Blavier et al., "The total carbon column observing network," *Philosophical Transactions of the Royal Society A: Mathematical, Physical and Engineering Sciences*, vol. 369, no. 1943, pp. 2087–2112, 2011.

[6] T. Warneke, Z. Yang, S. Olsen et al., "Seasonal and latitudinal variations of column averaged volume-mixing ratios of atmospheric CO_2," *Geophysical Research Letters*, vol. 32, no. 3, pp. 2–5, 2005.

[7] A. J. Cogan, H. Boesch, R. J. Parker et al., "Atmospheric carbon dioxide retrieved from the Greenhouse gases Observing SATellite (GOSAT): comparison with ground-based TCCON observations and GEOS-Chem model calculations," *Journal of Geophysical Research: Atmospheres*, vol. 117, no. 21, 2012.

[8] J. Messerschmidt, R. Macatangay, J. Notholt, T. Warneke, and C. Weinzierl, "Side by side measurements of CO_2 by ground-based Fourier transform spectrometry (FTS)," *Tellus B*, vol. 62, no. 5, pp. 749–758, 2010.

[9] R. Sussmann, A. Ostler, F. Forster et al., "First intercalibration of column-averaged methane from the total carbon column observing network and the network climate for the detection of atmospheric composition change," *Atmospheric Measurement Techniques*, vol. 6, no. 2, pp. 397–418, 2013.

[10] F. Hase, T. Blumenstock, and C. Paton-Walsh, "Analysis of the instrumental line shape of high-resolution Fourier transform IR spectrometers with gas cell measurements and new retrieval software," *Applied Optics*, vol. 38, no. 15, pp. 3417–3422, 1999.

[11] S. Dohe, V. Sherlock, F. Hase et al., "A method to correct sampling ghosts in historic near-infrared Fourier Transform Spectrometer (FTS) measurements," *Atmospheric Measurement Techniques*, vol. 6, no. 8, pp. 1981–1992, 2013.

[12] H. Tran, J.-M. Hartmann, G. Toon et al., "The $2v_3$ band of CH_4 revisited with line mixing: consequences for spectroscopy and atmospheric retrievals at 1.67 μm," *Journal of Quantitative Spectroscopy and Radiative Transfer*, vol. 111, no. 10, pp. 1344–1356, 2010.

[13] L. Kuai, D. Wunch, R.-L. Shia, B. Connor, C. Miller, and Y. Yung, "Vertically constrained CO_2 retrievals from TCCON measurements," *Journal of Quantitative Spectroscopy and Radiative Transfer*, vol. 113, no. 14, pp. 1753–1761, 2012.

[14] M. C. Geibel, C. Gerbig, and D. G. Feist, "A new fully automated FTIR system for total column measurements of greenhouse gases," *Atmospheric Measurement Techniques*, vol. 3, no. 5, pp. 1363–1375, 2010.

[15] Z. H. Yang, G. C. Toon, J. S. Margolis, and P. O. Wennberg, "Atmospheric CO_2 retrieved from ground-based near IR solar spectra," *Geophysical Research Letters*, vol. 29, no. 9, 2002.